# INGRID Analysis Technical Note

Masashi Otani
Akira Murakami
Christophe Bronner
for INGRID group

December 22, 2010

**Abstract**

In this note we summarize the INGRID analysis results with 2010a data. We measured the neutrino event rate, the beam profile center and these stability for the confirmation and support of 2010a oscillation analysis. We select the neutrino interaction, mainly charged current interaction, at each module and reconstruct the neutrino beam profile. We compare some distributions between data and MC and found good agreement. We get the data/MC ratio for the event rate to be $1.072 \pm 0.001$(stat.) $\pm$ 0.040(syst.). The center of the neutrino beam profile found to be $0.2 \pm 1.4$(stat.) $\pm$ 9.2(syst.) cm for X profile and -6.6 $\pm$ 1.5(stat.) $\pm$ 10.4(syst.) cm for Y profile. Finally the neutrino beam direction is measured to be $-0.22 \pm 0.37$ mrad as a direction from the beam origin to the center measured by INGRID.

# Contents

# Chapter 1

# Introduction

INGRID is on-axis near detector which consists of identical 14 modules [1] to monitor the beam stability. Each module has a sandwich structure made of the iron plates and the scintillator trackers.

We count the number of neutrino interactions, mainly CC interaction, at each module. The neutrino event rate is monitored and the profile is reconstructed. Fig.1.1 shows a typical event in an INGRID module. Detector coordinates are shown in the figure. INGRID uses a right-handed Cartesian coordinate system in which the z axis is the beam direction and the y axis is the vertical upward direction.

This article shows the measurements of

**(1)** neutrino event rate and its stability

**(2)** neutrino beam profile (center and width) and its stability

**(3)** neutrino beam direction

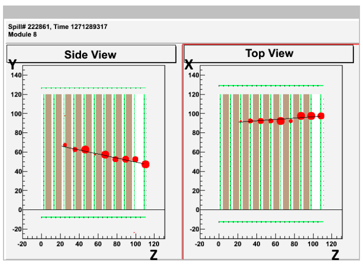


Figure 1.1: The typical neutrino event

[1] Additional two off-center modules and a proton module are installed after 2010a data taking.

This article is organized as follows. Chapter 2 explains the overview of Monte Carlo simulation and Chap.3 describes the data set of 2010a. Chapter 4 explains the neutrino event selection. Finally the result of the event rate measurement, beam profile measurement and beam direction are shown in Chap. 5, Chap. 6 and Chap. 7, respectively.

# Chapter 2

# Monte Carlo simulation

In this chapter, we explain Monte Carlo (MC) simulation used in this analysis.

We use three MC simulation programs : jnubeam, NEUT and detector simulation (Fig.2.1).

- Neutrino flux : jubeam (version 10d tuned ver. 2)
- Neutrino interaction to the target : NEUT (version 5.0.6.)
- Detector response simulation based on GEANT4 [1]

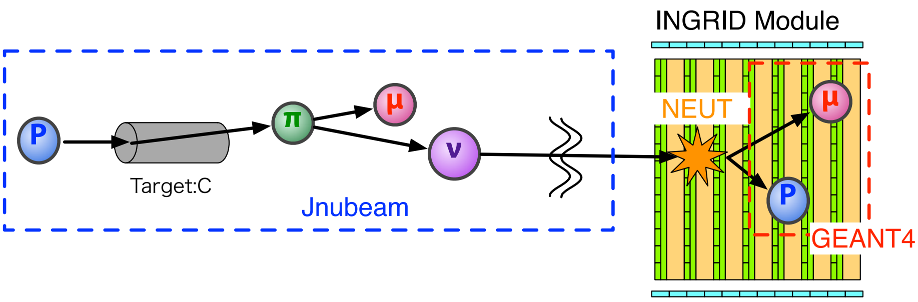


Figure 2.1: INGRID MC overview

### Neutrino flux prediction

Predictions for the neutrino flux are obtained via jnubeam version 10d. For a detailed description of jnubeam, see Ref.[1]. At the INGRID detector location a total neutrino flux per proton on target of *** $cm^{-2}$ is expected. Figure 2.2

[1]This INGRID MC is not the software of ND280 software packages

shows the energy spectrum at the INGRID center module, horizontal edge module and the Super-Kamiokande detector. Because each INGRID module covers the different off-axis angle, the neutrino energy spectrum is slightly different at each module. Table 2.1 shows the average neutrino energy at each module and the average energy is different for about ** GeV between the center module and the edge module.

Figure 2.2: Neutrino energy spectrum predicted by jnubeam

| module# | 0 | 1 | 2 | 3 | 4 | 5 | 6 | SK |
|---|---|---|---|---|---|---|---|---|
| Average energy[GeV] | | | | | | | | |

Table 2.1: Average neutrino energy

**Neutrino interaction simulation**

We simulate neutrino interactions with target iron plate (Fe) in the INGRID detector with the NEUT program libraries. Currently, we simulate all the neutrino interaction with iron (Fe) as the target nuclei, although INGRID consists of iron, scintillator and support material. Simulation with correct material is under preparation. For a detailed description of NEUT, see Ref.[2].

**Detector response simulation**

We simulate the detector response to the generated particles from the neutrino interaction with simulator based on GEANT4. We obtain the x and y position of the neutrino interaction from jubeam flux file. The vertex z is uniformly generated in the iron plate and the scintillator tacker taking into account the mass ratio of iron planes (99.54 ton) to scintillator planes (3.74 ton).

Detector response simulation includes following effects which have an impact to the efficiency to the neutrino interactions.

- We tuned the conversion factor from energy deposit to number of photon in MC simulation by adjusting the peak PE of beam related sand muon. We also include the quenching effect of scintillator, attenuation of photon propagating in the fiber and MPPC response model (we refer [**?**] Figure 2.3 shows the typical PE distribution of beam related sand muon after these MC tuning.

- Although the inefficiency resulted from the photoelectron statistics (light yield is $\sim$ 30 PE at peak and threshold is 2.5 PE) is expected to be small (less than 0.1%), each channel has 1 $\sim$ 2% inefficiency resulted from the gap between scintillator bars, which is studied by cosmic-ray data. Figure 2.4 black line shows the tracking inefficiency of data. Because the particle with low angle can go through the gap easily, the inefficiency become larger to the low angle track. We tuned the cross-section of the scintillator bar in MC with real geometry (Fig.2.5) to reproduce the angular dependence of the inefficiency in data (Fig.2.4 blue and red).

- Accidental hits by MPPC dark noise result in miss reconstruction of the track, miss identification of the vertex position. In consequence the selection efficiency is influenced by MPPC dark noise. In MC the MPPC noise hit is generated to reproduce the number of PE, timing, and noise rate of data (Fig.2.6 shows the timing distribution).

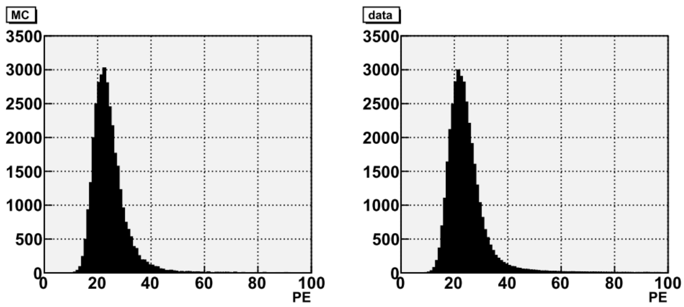


Figure 2.3: PE distribution of beam related sand muon. Left plot is MC simulation and right one is data.

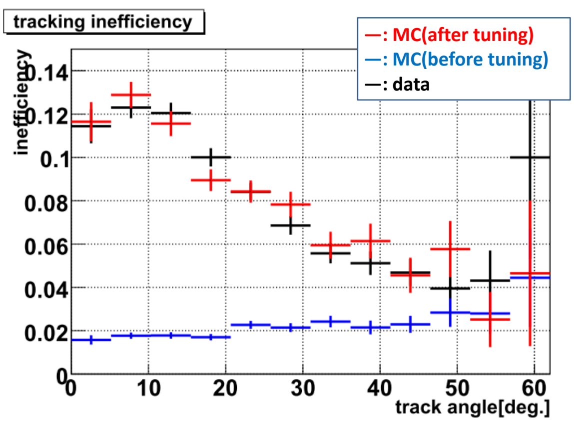


Figure 2.4: Tracking inefficiency as a function of angle of the reconstructed track

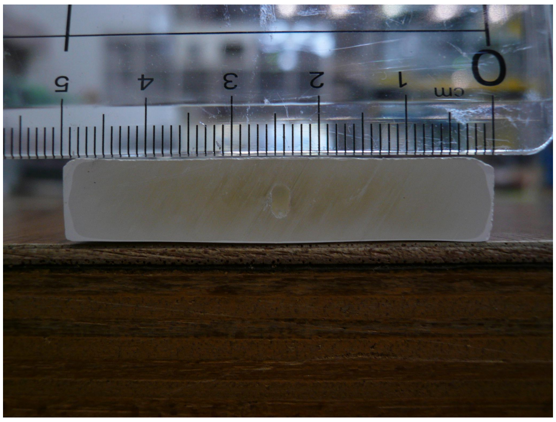

Figure 2.5: Photo of the cross-section of the scintillator bar

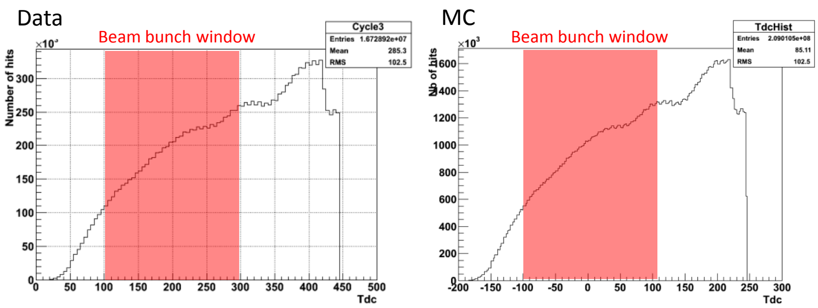


Figure 2.6: The timing distribution of MPPC noise. left is data and right is MC.

# Chapter 3

# Data set

We took beam data from January to June, 2010. Data taking period, number of good spills and number of INGRID good spills are summazied int Table 3.1. Data taking efficiency for entire period is 99.9%, and total number of delivered protons is $3.255 \times 10^{19}$. The MC simulation corresponds to an equivalent of $100 \times 10^{21}$ pot.

| MR run # | Period | Good spills | INGRID good spills | Protons at CT05 |
|---|---|---|---|---|
| 29 | Jan. 23 - Feb. 5 | 26813 | 26813 | $0.32 \times 10^{18}$ |
| 30 | Feb. 24 - Feb. 28 | 59256 | 59070 | $1.12 \times 10^{18}$ |
| 31 | Mar. 19 - Mar. 25 | 86980 | 86935 | $1.97 \times 10^{18}$ |
| 32 | Arp. 14 - May. 1 | 237350 | 236647 | $7.64 \times 10^{18}$ |
| 33 | May. 9 - Jun. 1 | 350079 | 350012 | $1.22 \times 10^{19}$ |
| 34 | Jun. 7 - Jun. 26 | 246504 | 246410 | $9.30 \times 10^{18}$ |
| Total | | 1006982 | 1005887 | $3.26 \times 10^{19}$ |

Table 3.1: Summary of data sets

# Chapter 4

# Neutrino event selection

## 4.1 Event selection

We select a long track of charged particle started within the fiducial volume of an INGRID module to select the neutrino interaction. Before reconstruction of the track, plane activity and PE cut are applied to reject an accidental noise event. After reconstruction of the track, VETO cut and fiducial cut are applied to reject the incoming particle from the neutrino interaction at upstream materials. The order of the event selections is shown below.

**(1)** Time clustering

**(2)** Number of active planes $> 2$

**(3)** PE/active layer $> 6.5$

**(4)** Tracking

**(5)** Track matching

**(6)** Beam timing cut

**(7)** Upstream VETO cut

**(8)** Fiducial volume cut

All the selections are done a module by module and bunch by bunch basis. In this analysis, the channel which has a ADC signal larger than 2.5 PE, which corresponds to TDC threshold, is defined as the hit.

At the first step hits are clustered with following criteria; If there are more than 3 hits within 100 nsec, all the hits within $\pm$ 50 nsec from the mean time are brought together into a cluster. Within the cluster the number of planes with at least one coincidence hit in a both x and y layers [1] , which are called

[1] INGRID module consists 11 planes and the plane consists 2 layers. Each layer has 24 scitillator bars and the direction of scitillator is perpendicular each other layer.

active layers, is counted. Figure 4.1 shows the distribution of the number of planes with the active layers, which are called active planes, and Fig.4.2 shows total PE of all hits in the active layer divided by the number of active layers (PE/(number of active layers)). The event with more than 2 active planes and more than 6.5 PE/(number of active layers) is selected.

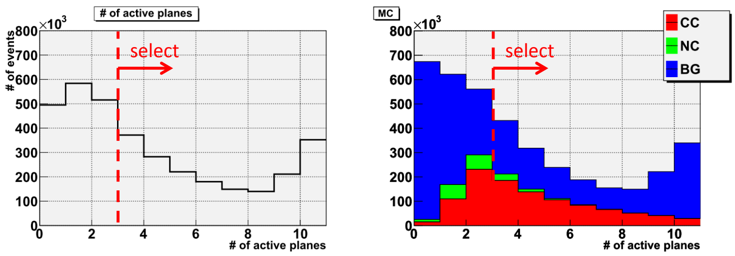


Figure 4.1: The number of active planes(left:DATA, right:MC normalized by area)

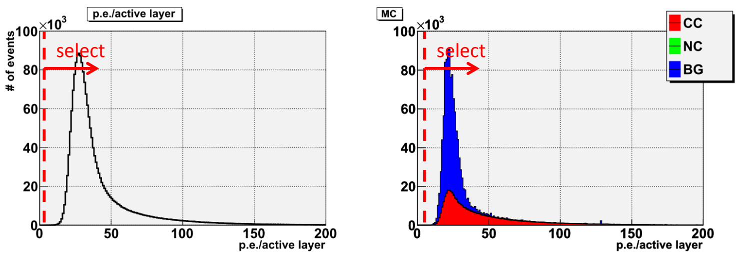


Figure 4.2: PE/(number of active layers) (left:DATA, right:MC normalized by area)

After these selections track is reconstructed. First the hits in the most downstream active plane are adopted as end-point of the track. Looking at the hits in next upstream plane in order, the hit is selected as track if calculated slope is matched with straight line.

After reconstruction of the track some badly fitted tracks are rejected by considering the difference of vertex z between a 2-D track in x view and y view. Fig.4.3 shows the distribution of the difference of the vertex z between 2-D track in x view and y view. We require the difference is smaller than 2 planes. Figure 4.4 shows the angular distribution of the reconstructed track.

Because there are some background events such as cosmic-ray on beam off timing, the events within ± 100 nsec from the expected timing of each bunch are selected (Fig.4.5).

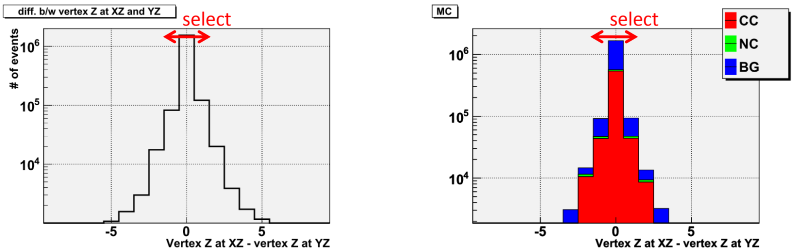


Figure 4.3: Difference of the vertex z in X-view and Y-view(left:DATA, right:MC normalized by area)

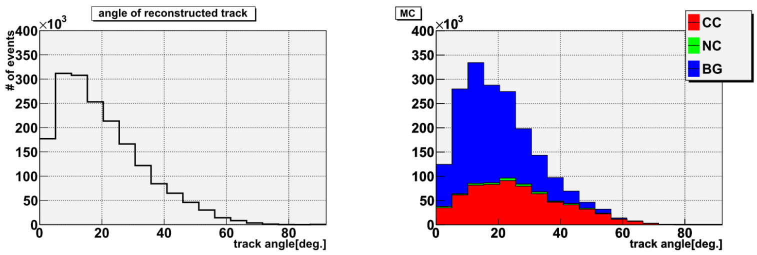


Figure 4.4: Angle of reconstructed track(left:DATA, right:MC normalized by area)

Finally we apply two selections to reject the incoming particles produced by the neutrino interaction in upstream materials. First one is upstream VETO selection. If the VETO plane has a hit at the position expected from extrapolation to upstream with the reconstructed track, its event is rejected. Figure 4.6 shows the example of the event rejected at this selection. After that we apply fiducial volume cut. The fiducial volume is the cubic volume which is defined as ± 50 cm from the center of an INGRID module (Fig.4.7). The position of most upstream hit associated with the reconstructed track is applied as the vertex and we require that vertex is in the fiducial volume (Fig.4.8 and 4.9).

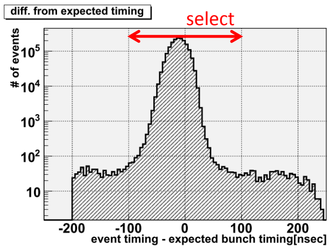


Figure 4.5: Time residual plot

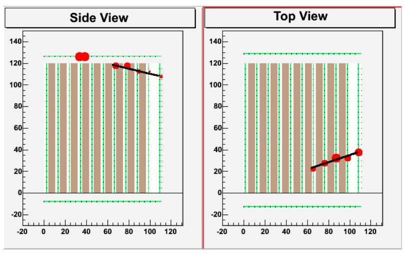


Figure 4.6: The event rejected by upstream VETO selection

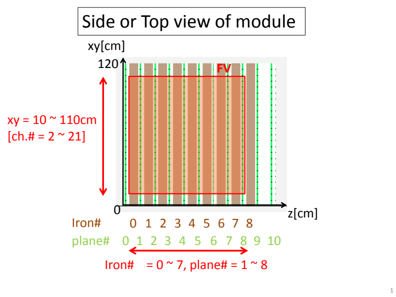


Figure 4.7: The definition of fiducial volume

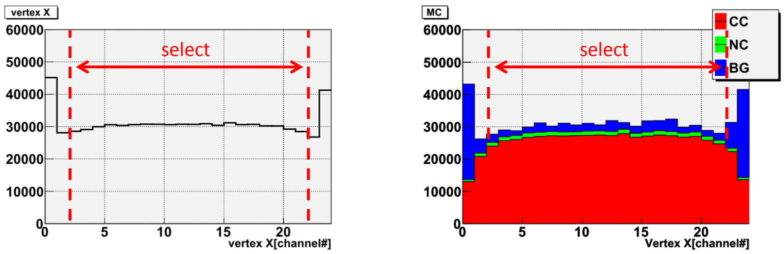


Figure 4.8: vertex x(left:DATA, right:MC normalized by area)

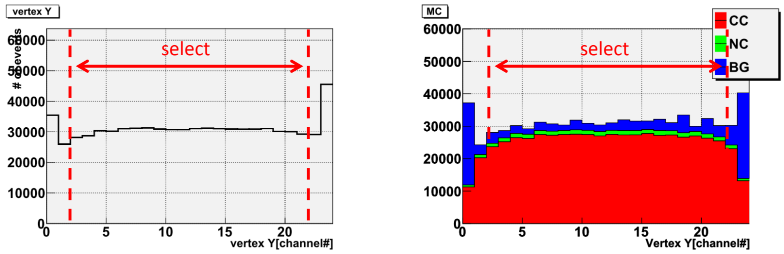


Figure 4.9: vertex y(left:DATA, right:MC normalized by area)

### Event selection summary

The number of events and the selection efficiencies at each selection step is summarized in Tab.4.1. We obtained 493813 neutrino event candidates among 2010a data set.

| | selection | Data | selection eff. | MC | selection eff. |
|---|---|---|---|---|---|
| 1 | # of active planes > 2 | 1906146 | | $1.97 \times 10^6$ | |
| 2 | PE / active layers > 6.5 | 1906078 | (1.00) | $1.97 \times 10^6$ | (1.00) |
| 3 | Tracking | 1804786 | (0.95) | $1.83 \times 10^6$ | (0.93) |
| 4 | Track matching | 1749548 | (0.97) | $1.77 \times 10^6$ | (0.97) |
| 5 | Beam timing | 1747181 | (0.99) | $1.77 \times 10^6$ | (1.00) |
| 6 | Upstream VETO cut | 745912 | (0.43) | $7.35 \times 10^5$ | (0.42) |
| 7 | Vertex in fiducial | 493813 | (0.66) | $4.75 \times 10^5$ | (0.66) |

Table 4.1: Summary of the event selection. Data and MC are normalized by pot

## 4.2 Basic distribution of data and MC simulation

In this section we show some distributions of the selected events. In each distribution, there are two plots; one is data and MC simulation overlaid and one is data/MC. In each plot the distribution of MC simulation is normalized by the area of the distribution of data. The data/MC ratio is within few percents at each plot and we found good agreement between DATA and MC.

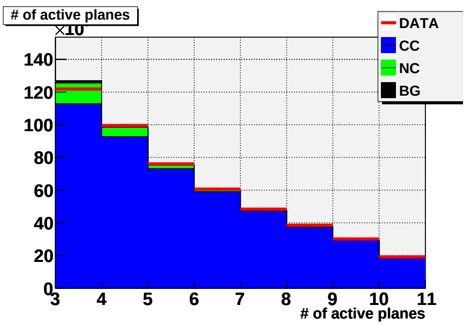


Figure 4.10: number of active planes

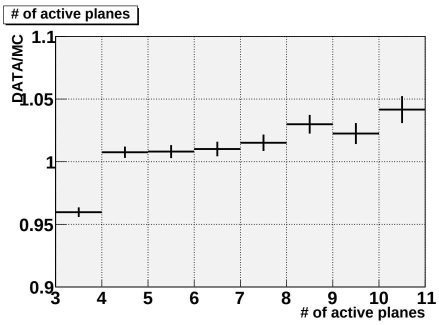


Figure 4.11: DATA/MC

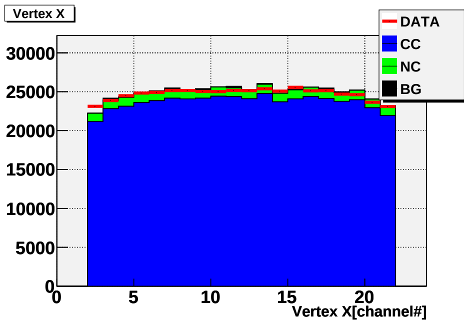


Figure 4.12: Vertex X

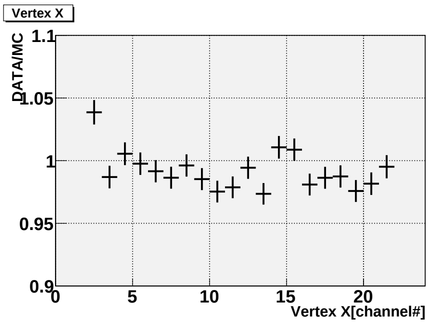


Figure 4.13: DATA/MC

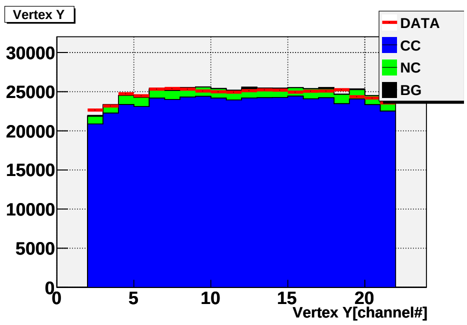


Figure 4.14: Vertex Y

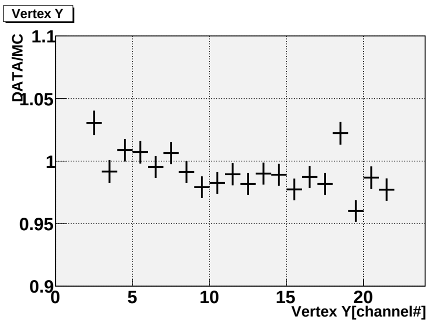


Figure 4.15: DATA/MC

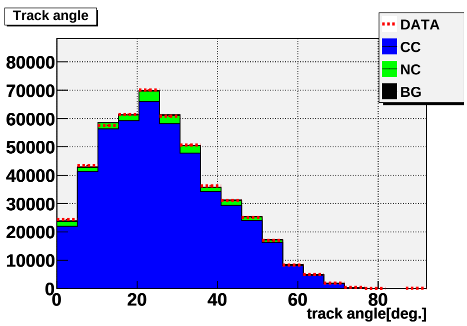


Figure 4.16: Reconstructed track angle

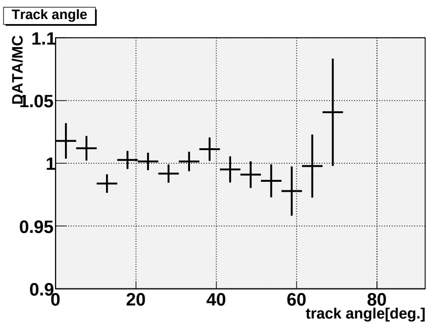


Figure 4.17: DATA/MC

## 4.3 Reconstruction resolution

Reconstruction resolution is checked by MC simulation to compare the reconstructed value and the MC true information. The results of vertex X, Y and track angle are shown in Fig.4.18, Fig.4.19 and 4.20, respectively. Their r.m.s. for CCQE events are 2.7 cm for X, 2.8 cm for Y and 3.8 degree, respectively.

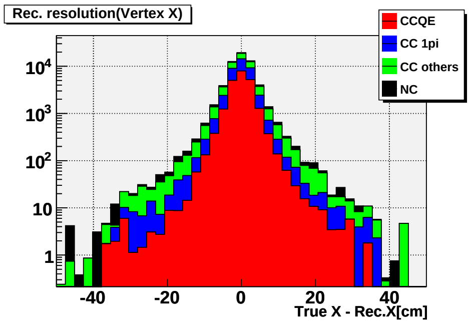


Figure 4.18: X resolution

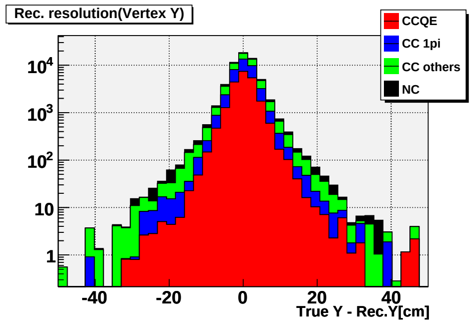


Figure 4.19: Y resolution

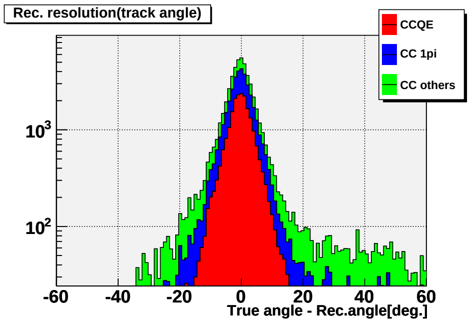


Figure 4.20: Angular resolution of reconstructed track

## 4.4 Efficiency to neutrino interaction

The event selection efficiency as a function of true neutrino energy is shown in Fig.4.21 and 4.22. Here, the efficiency is defined as the ratio of the number of selected events to that of the events generated inside the fiducial volume. Figure 4.23 shows the selection efficiency for CC interactions as a function of the muon angle. Because the acceptance for the muon angle and the muon angle depends the neutrino energy (Fig.4.24), the efficiency for CC interaction depends the neutrino energy. Figure 4.25 shows the efficiency for the muon with various angle and low angle (less than 15 degrees). The selection efficiency for the muon with low angle is almost 100% and the rising edge around 0.3 GeV corresponds to the minimum energy of the muon to penetrate the 2 iron plates and 3 scintillator trackers.

Table 4.2 shows the selection efficiency for each module. Because the energy spectrum of the beam neutrino is slightly different module by module, the selection efficiency is also different.

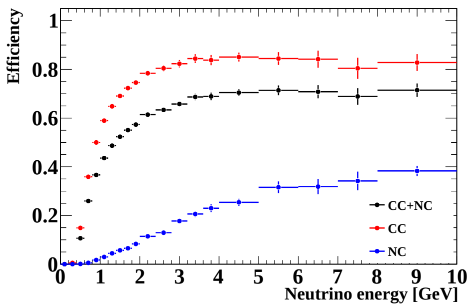


Figure 4.21: Neutrino event selection efficiency

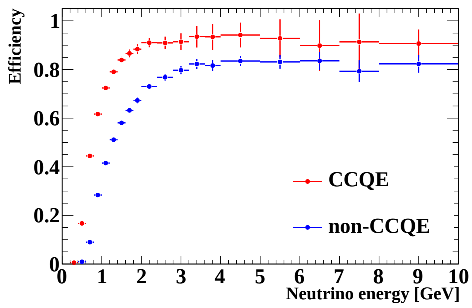


Figure 4.22: Selection efficiency for CCQE and CC others.

| module | Mean efficiency[% ] |
|---|---|
| 0 | 51.7 |
| 1 | 54.0 |
| 2 | 55.1 |
| 3 | 55.1 |
| 4 | 55.0 |
| 5 | 54.2 |
| 6 | 51.2 |

Table 4.2: Mean efficiency of each module

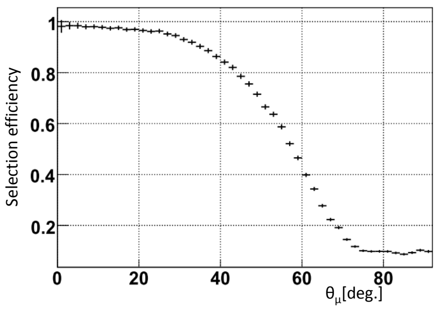


Figure 4.23: The selection efficiency for CC interactions as a function of the muon angle.

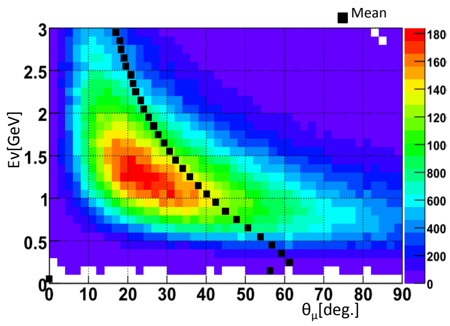


Figure 4.24: The neutrino energy VS. the muon angle generated from CC interactions

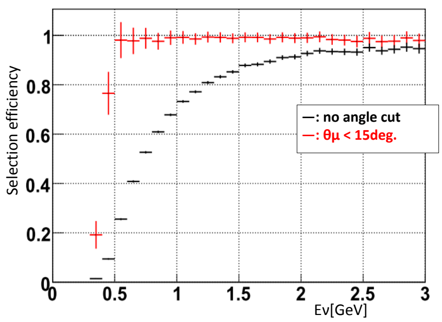


Figure 4.25: The selection efficiency for CC interactions for the muon with various angle and low angle

# Chapter 5

# Event rate measurement

## 5.1 Event rate stability

Fig.5.1 shows daily event rate normalized by delivered pot. We succeeded to measure the daily event rate with about 1.7% statistical error each day. The chi-square calculated from the average rate is 86 for 76 degrees of freedom. It is concluded that the beam events is stable within statistical error.

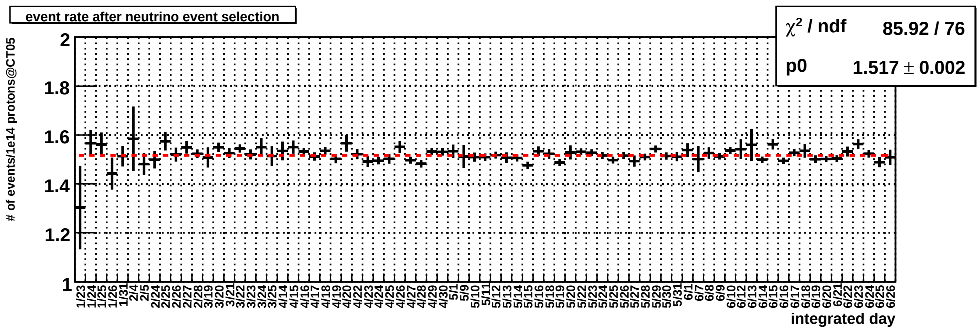


Figure 5.1: The stability of daily event rate

## 5.2 data/MC of event rate

To obtain the number of events in the fiducial volume ($N^{obs.}$), we need to do following corrections.

**(1)** Accidental MPPC noise

**(2)** Iron mass

**(3)** Beam related background

Detail description is in Chap. A.

We derive the formula to evaluate the number of events in the fiducial volume from number of selected events ($N^{sel.}$); $N^{obs.} = N^{sel.} \times \frac{1}{1+C}$, where C is the correction factor. The corrected number of events are summarized in Table 5.1 respectively. Detail for it is summarized in Chap. A. Finally we obtain DATA/MC to be 1.072 $\pm$ 0.001 (stat.).

| | |
|---|---|
| Number of selected events | 493813 |
| Corrected number of events | 508511 |

Table 5.1: Number of events before and after corrections

## 5.3 Systematic error of event rate

Table 5.2 shows the systematic errors which does not include physics uncertainty such as neutrino cross-section.

| Item | Error[%] |
|---|---|
| Accidental MPPC noise | 0.7 |
| Iron mass | 0.1 |
| Beam related background | 0.2 |
| Fiducial selection | 1.1 |
| Hit efficiency | 1.8 |
| Tracking efficiency | 1.4 |
| Track matching selection | 2.7 |
| Not beam-related background | <0.1 |
| p.e./active layer selection | <0.1 |
| Beam timing selection | <0.1 |
| Total | 3.7 |

Table 5.2: Systematic error table

### Accidental MPPC noise

The effect of MPPC noise is studied with MC in which the MPPC noise hit is generated to reproduce number of PE, timing, and noise rate of DATA. We found that the more MPPC noise rate is, the more neutrino events are lost due to miss identification of vertex Z or miss counting of number of active planes. Its effect is found to be linear and slope is estimated to be -0.9585 %. Two sources of systematic errors are considered. First one comes from the error on the linear fit. To get this systematic error, we multiply the fit error by the maximal measured noise rate. Second one comes from the measurement of noise. Correction factors are calculated using the average noise rate measured on one period. But this noise rate fluctuates in time (probably due to temperature variations). So we measure the maximal difference between average noise rate and noise rate measured at different times during one period, and using the linear relation between noise rate and variation of number of events we get the systematic error. The quadratic sum of these two errors is 0.7 %.

### Iron mass

Before construction of INGRID the mass of each iron plate was measured with a precision of 1 kg, which corresponds to 0.13 % of the mass of one iron plate. We will use this figure as the systematic error on this correction factor. We might need to increase this systematic error in the future, as the correction factors are calculated using the mass of the whole iron plate, when we actually use a fiducial cut in analysis, only interactions in the central part of the iron plates are kept.

### Beam-related background

We estimated the contamination fraction of beam related background with wall neutrino Monte Carlo. The fraction is estimated to be 0.4% , in which the number of interactions of background is normalized to compare the number of dirt muon in DATA and MC. There is a 35% difference from POT expectation, which is considered as one of the source of the systematic error. We considered 20% neutrino flux uncertainty and 20% cross section uncertainty as other sources of the systematic error. Finally 0.2% ($=\sqrt{0.35^2 + 0.2^2 + 0.2^2}$) is applied as the systematic error.

### Fiducial selection

To estimate the uncertainty of fiducial selection and the effect of non uniformity of iron plate, we divided fiducial in several horizontal slices and checked the difference between DATA and MC. Table 5.3 shows the result. The maximum absolute value, 1.1%, is applied as systematic error.

| selection | DATA | MC | \|DATA - MC\| |
|---|---|---|---|
| <50 cm from center(nominal selection) | 100.0 | 100.0 | 0.0 |
| <25 cm | 25.6 | 25.2 | 0.4 |
| 25 $\sim$ 40 cm | 39.9 | 39.3 | 0.6 |
| 40 $\sim$ 50 cm | 34.4 | 35.5 | 1.1 |
| Systematic error ( Maximum absolute ) | | | 1.1 |

Table 5.3: DATA-MC for several sub fiducial volume

### Hit efficiency

We estimated the relation between hit efficiency and number of selected events with MC. Fig. 5.2 shows the result from which the systematic error of hit efficiency is estimated to be 1.8% because hit efficiency has 1.1% uncertainty. [1]

### Track matching selection

In the neutrino event selection, after reconstruction of XZ track and YZ track we require track start point matching. To estimate the uncertainty of the selection, we changed the tolerance for the matching and checked the difference of the number of selected events between DATA and MC. Table 5.4 shows the result. The maximum absolute value, 2.7%, is applied as systematic error.

[1] 0.5% of the measurement error of hit efficiency, 1.0% of the tuning of hit efficiency in MC

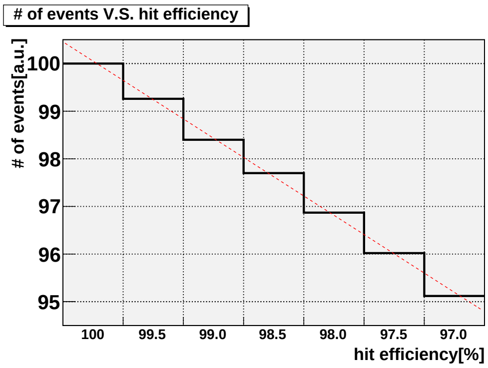


Figure 5.2: hit efficiency V.S. number of selected events

| Vertex Z of XZ track - Vertex Z of YZ track | DATA | MC | \|DATA - MC\| |
|---|---|---|---|
| -1, 0, +1 (nominal selection) | 100.0 | 100.0 | 0.0 |
| 0 | 83.0 | 85.7 | 2.7 |
| -2, -1, 0, +1, +2 | 104.0 | 103.0 | 1.0 |
| Systematic error ( Maximum ) | | | 2.7 |

Table 5.4: DATA-MC for several tolerance of track matching.

### Tracking efficiency

To check the difference of the tracking efficiency between DATA and MC, the tracking efficiency is compared with several sub-sample selected by number of active planes. Table 5.5 shows the result. The maximum absolute value, 1.4%, is applied as systematic error.

### Not beam-related background

The off-bunch data (cycle 17 $\sim$ 22 where as on-bunch cycle is 4 $\sim$ 9) are analyzed with same procedure and only 93 events are selected whereas the number of signal is 493813. It is negligible.

### PE/active layer selection

To estimate the uncertainty of PE/active layer selection, we changed the cut value and checked the difference of number of selected events from one with nominal cut. The result is the difference is less than 0.01% and its uncertainty is negligible.

| number of active planes | DATA | MC | \|DATA - MC\| |
|---|---|---|---|
| 3 | 87.6 | 86.9 | 0.7 |
| 4 | 93.2 | 91.8 | 1.4 |
| 5 | 94.7 | 94.3 | 0.5 |
| 6 | 95.6 | 96.2 | 0.6 |
| 7 | 96.2 | 96.6 | 0.4 |
| 8 | 96.7 | 96.8 | 0.1 |
| 9 | 98.7 | 97.9 | 0.8 |
| 10 | 99.1 | 99.0 | 0.1 |
| Systematic error ( Maximum ) | | | 1.4 |

Table 5.5: The tracking efficiency of DATA and MC with several sub sample

**beam timing selection**

To estimate the uncertainty from neutrino beam timing, we changed the cut value and checked the difference of number of events from nominal cut. The difference is less than 0.01% and it is negligible.

# Chapter 6

# Measurement of beam profile

## 6.1 Stability of beam profile

Fig.6.1 shows horizontal and vertical beam profile with RUN 32 data. Fitted center with gaussian is $0.1 \pm 2.9$ cm for horizontal and $-10.9 \pm 3.2$ cm for vertical. Fig.6.4 and 6.5 show the monthly beam center of horizontal and vertical respectively. We succeeded to measure the profile center with about 4.2 cm statistical error for each month. The chi-square is calculated to be almost one to the degree of freedom (0.8 for X and Y center). It is concluded that the beam profile center is stable within statistical error.

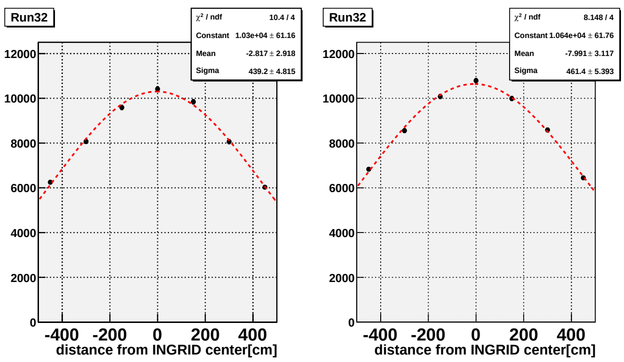


Figure 6.1: Horizontal profile(left) and vertical profile(right)

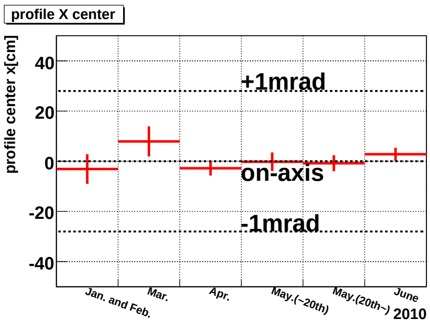


Figure 6.2: Horizontal profile center.

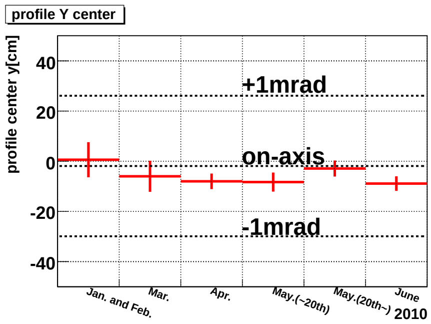


Figure 6.3: Vertical profile center

## 6.2 The systematic error of beam center

We estimated the systematic error with toy profile MC in which the number of events at each module is varied with 3.7% from original profile made by RUN 29 34 all data. 100'000 profiles are generated and the RMS of fitted center is applied as systematic error. The result shows 9.2 cm (0.33 mrad) for horizontal center and 10.4 cm (0.37 mrad) for vertical center.

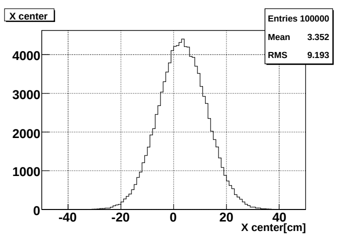


Figure 6.4: Fitted Horizontal center with 100'000 profiles

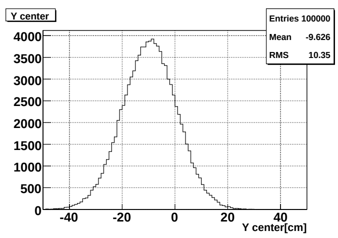


Figure 6.5: Fitted Vertical center with 100'000 profiles

# Chapter 7

# Measurement of beam direction

# Chapter 8

# Conclusion

In this note we have presented the measurement of the neutrino event rate and profile center in INGRID durint 2010a. We selected the neutrino interactions to reconstruct the long track started within fiducial volume. The results have been compared to MC and found good agreement with DATA. Finally DATA/MC of the event rate and beam profile centers have been evaluated with an associated systematic error:

$$\begin{aligned} \mathrm{R}_{\mathrm{DATA/MC}} &= 1.072 \pm 0.001(\mathrm{stat.}) \pm 0.040(\mathrm{syst.}) & \\ \mathrm{Xcenter} &= +0.2 \pm 1.4(\mathrm{stat}) \pm 9.2(\mathrm{syst.}) & \mathrm{cm} \\ \mathrm{Ycenter} &= -6.6 \pm 1.5(\mathrm{stat.}) \pm 10.4(\mathrm{syst}) & \mathrm{cm} \end{aligned}$$

# Appendix A

# Correction factors for neutrino event rate

### Iron mass

In INGRID most of the neutrino interactions occur in the 9 iron targets of each module. During their fabrication, there was a tolerance on the thickness of those iron planes. This results in iron planes having slightly different volumes, and as a consequence different masses. The maximal variation from design mass is 2.15 % from the given tolerance on thickness. The mass of each iron plane was measured at the end of the fabrication process, so we can deduce correction factors for the expected number of events for each module, by using the fact that 95.2 % of interactions in one module occur in the iron.

### Accidental MPPC noise

Another correction on the number of observed events comes from noise hits in the detector. Those noise hits reduce the number of reconstructed events compared to the case when there is no noise. To correct this effect, we use the following procedure:

**(1)** Measure noise in data

**(2)** Create a noise simulation to reproduce those measurements

**(3)** Use Monte Carlo simulation to compare the number of reconstructed events with and without adding noise

**(4)** Deduce from the simulation correction factors and systematic errors

Noise is measured in beam data. We measure the rate of noise hits, which are defined as hits occuring in the detector when no particles are actually going through the detector. To find such hits, we look at cycles where beam spills are not coming (INGRID records data on 23 integration cycles, but beam spills only arrive during 6 of them), and perform regular event selection to make sure there is no cosmic particle in the detector. We then measure a noise rate for each channel of the detector, as well as light yield and timing distribution.

Noise is then simulated with a given probability for each channel. Timing for the noise hits is simulated using the distribution measured in data. Light yield is then simulated using a measured light yield distribution for the corresponding timing.

Monte Carlo simulation is then used to measure the variation of number of reconstructed events due to noise. We first reconstruct events on Monte Carlo files which do not include noise hits, then add noise hits to those files and perform reconstruction again. We then compare the number of reconstructed events in each case. The simulation is using jnubeam 10c.

From this simulation we have for each module a noise rate and the variation of number of reconstructed events due to noise. There is a linear relation between them as can be seen on Fig.A.1. We will use this linear relation to make corrections on the number of observed events. This relation is:

$$\text{Variation of number of events [\%]} = -0.9585 * < \text{noise rate} >$$

Those corrections are made for each module, and each subset of events we are considering. In each case we measure the noise rate, and then from the linear relation deduce the variation of number of reconstructed events which should be used as a correction factor.

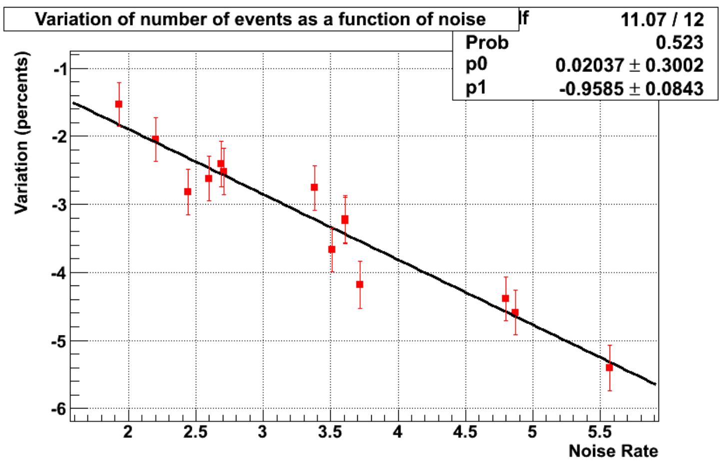


Figure A.1: Variation of number of reconstructed events as a function of noise rate

## Beam related background

We estimated the contamination fraction of beam related background with background MC in which neutrino and the interaction is generated in upstream dirt ( 10 x 10 x 5 $m^3$).

Almost all contaminations come from short track induced neutron ($\sim 50\%$) or gamma ($\sim 40\%$) and dirt muon ($\sim 10\%$) which is not detected accidentally due to scintillator inefficiency.

In background MC, number of generated interactions is normalized so that number of rejected events at upstream VETO selection, which consists dirt muon mainly, is equal to DATA and MC. The difference from POT expectation is 35% and it is considered as systematic error. Finally contamination fraction is estimated to be 0.4% and it is applied as one of the correction factor.

## Summary of the correction factor

Run by run and module by module correction factors are summarized int Table A.1

| | module | 29,30 | 31 | 32 | 33 | 33 | 34 |
|---|---|---|---|---|---|---|---|
| number of events | 0 | 1054 | 1548 | 5956 | 4119 | 5425 | 6962 |
| | 1 | 1526 | 2033 | 7827 | 5432 | 7122 | 9520 |
| | 2 | 1875 | 2476 | 9360 | 6492 | 8555 | 11622 |
| | 3 | 1882 | 2570 | 10133 | 6795 | 9078 | 12191 |
| | 4 | 1831 | 2459 | 9627 | 6636 | 8683 | 11651 |
| | 5 | 1524 | 2176 | 7876 | 5421 | 7217 | 9588 |
| | 6 | 1058 | 1585 | 5837 | 4172 | 5421 | 7285 |
| | 7 | 1229 | 1717 | 6636 | 4509 | 5826 | 8100 |
| | 8 | 1588 | 2187 | 8351 | 5819 | 7620 | 10270 |
| | 9 | 1884 | 2562 | 9770 | 6632 | 8766 | 11946 |
| | 10 | 1949 | 2681 | 10305 | 6987 | 9373 | 12473 |
| | 11 | 1908 | 2520 | 9771 | 6713 | 8897 | 11871 |
| | 12 | 1561 | 2133 | 8146 | 5512 | 7193 | 9822 |
| | 13 | 1218 | 1659 | 6263 | 4327 | 5815 | 7734 |
| correction factor | 0 | -3.3 | -3.3 | -4.3 | -4.0 | -3.9 | -3.9 |
| | 1 | -2.6 | -2.6 | -2.6 | -2.4 | -2.4 | -2.4 |
| | 2 | -2.0 | -2.0 | -2.0 | -1.7 | -1.7 | -1.7 |
| | 3 | -2.3 | -2.3 | -2.3 | -2.0 | -1.9 | -1.9 |
| | 4 | -1.8 | -1.8 | -1.8 | -1.6 | -1.5 | -1.5 |
| | 5 | -1.9 | -1.9 | -1.9 | -1.6 | -1.5 | -1.4 |
| | 6 | -2.3 | -2.3 | -2.8 | -2.5 | -2.4 | -2.3 |
| | 7 | -2.7 | -2.7 | -2.5 | -3.5 | -3.3 | -3.1 |
| | 8 | -2.2 | -2.2 | -2.0 | -3.0 | -2.8 | -2.6 |
| | 9 | -2.1 | -2.1 | -2.7 | -4.1 | -3.8 | -3.6 |
| | 10 | -4.2 | -4.2 | -4.1 | -5.4 | -5.2 | -5.0 |
| | 11 | -1.9 | -1.9 | -1.8 | -2.9 | -2.7 | -2.6 |
| | 12 | -4.9 | -4.9 | -4.7 | -6.2 | -6.0 | -5.9 |
| | 13 | -2.5 | -2.5 | -2.5 | -3.4 | -3.2 | -3.0 |
| Number of cor. | 0 | 1090 | 1601 | 6224 | 4292 | 5647 | 7242 |
| | 1 | 1567 | 2087 | 8037 | 5565 | 7298 | 9756 |
| | 2 | 1913 | 2526 | 9551 | 6606 | 8703 | 11822 |
| | 3 | 1927 | 2632 | 10374 | 6934 | 9255 | 12422 |
| | 4 | 1865 | 2504 | 9804 | 6741 | 8817 | 11825 |
| | 5 | 1553 | 2218 | 8028 | 5509 | 7328 | 9697 |
| | 6 | 1083 | 1622 | 6002 | 4278 | 5552 | 7453 |
| | 7 | 1263 | 1765 | 6803 | 4674 | 6024 | 8360 |
| | 8 | 1624 | 2237 | 8520 | 6001 | 7838 | 10545 |
| | 9 | 1925 | 2617 | 10040 | 6912 | 9110 | 12391 |
| | 10 | 2035 | 2800 | 10742 | 7385 | 9883 | 13130 |
| | 11 | 1945 | 2569 | 9951 | 6914 | 9143 | 12183 |
| | 12 | 1641 | 2242 | 8550 | 5878 | 7653 | 10435 |
| | 13 | 1250 | 1702 | 6421 | 4478 | 6005 | 7976 |

Table A.1: Correction factors

# Bibliography

[1] will be put the name of jnubeam tech. note

[2] will be put the name of NEUT doc.

[3] the report by Calibration group of ND280 working group put on http://www.t2k.org/nd280/calib/Meetings/Jan10Workshop/MPPClinearity/at_download/filet2k.org).